Deployment and Performance of a Broadband Seismic Network near the New Korean Jang Bogo Research Station, Terra Nova Bay, East Antarctica

by Yongcheol Park, Hyun Jae Yoo, Won Sang Lee, Joohan Lee, Yeadong Kim, Sang-Hyun Lee, Dongseob Shin, and Hadong Park

INTRODUCTION

The Republic of Korea first constructed a permanent year-round base named King Sejong Station on King George Island near the northern Antarctic Peninsula in 1988 (inset map in Fig. 1). Given the distance from the Antarctic continent, however, the extent of in-depth research and international collaboration at this first station has been limited. In this context, construction of a second scientific research station on the mainland of Antarctica was proposed in 2004 (Hong et al., 2005), and six candidate sites were selected in 2007 (Lee et al., 2012). Korean government experts, including scientists from the KOPRI (Lee et al., 2012), conducted field investigations and assessed the candidate sites from 2007 to early 2010. Considering the research planned for the new station, the potential environmental impact, logistical convenience, and existing international research network, the assessment and three open hearings held in Korea resulted in selection of the final site on the coast of Terra Nova Bay (TNB; 74°37.4′ S, 164°13.7′ E) in northern Victoria Land (Fig. 1). A paper supporting this choice was submitted to the XXXIII Antarctic Treaty Consultative Meeting held in Punta del Este, Uruguay, in May 2010. The station was named Jang Bogo, after a distinguished figure in Korean history who built the marine Silk Road to enable the international exchange of goods and culture in the ninth century. In TNB, there is an Italian summer research station, Mario Zucchelli station, which is ~10 km away to the southwest from Jang Bogo Station (Fig. 1), and we visited the station by helicopter from the construction site of Jang Bogo Station to discuss future research and sharing facilities.

A comprehensive environmental evaluation was performed from 2011 to 2012 to minimize adverse impacts of the construction and operation of Jang Bogo. During that period, the Extreme Geophysics Group from the KOPRI initially installed four broadband seismic stations surrounding Mt. Melbourne to monitor its volcanic activity. The seismic network was named the Korea Polar Seismic Network at TNB (KPSN@TNB). This paper reports on the development of KPSN@TNB under the harsh Antarctic conditions and its operation and evolution.

TECTONIC SETTING OF THE TERRA NOVA BAY REGION

Jang Bogo Station is located in Victoria Land on the eastern flank of the Ross Sea rift, part of the West Antarctic rift system, one of the several large tectonic provinces of the Earth formed by the Cretaceous to Cenozoic extension (blue dotted line in the inset map in Fig. 1). The rift shoulder consists of the Transantarctic Mountains, which form the morphological and geological boundary between East and West Antarctica (Behrendt and Cooper, 1991; Rocchi et al., 2002) (light gray line in the inset in Fig. 1). Various models have been suggested to explain the uplift of the Transantarctic Mountains. These include thermal conduction or advection from the hotter West Antarctic lithosphere to that of cooler East Antarctica (Behrendt, 1999) or from a hot mantle anomaly (e.g., Berg et al., 1989; Danesi and Morelli, 2001; Faccenna et al., 2008; Lawrence et al., 2006; Smith and Drewry, 1984). Others include flexural uplift of the edge of East Antarctica (ten Brink and Stern, 1992; ten Brink et al., 1997) or an asymmetric rifting model defined by a shallow crustal penetrative detachment zone dipping westward beneath the Transantarctic Mountains (Fitzgerald et al., 1986). Although many models have been proposed, the cause of uplift is still debated, but it is likely related to the activity of the West Antarctic rift system. In addition to the continental scale of tectonics, many interesting regional features are nearby, including the Mt. Melbourne volcano and the Campbell and Priestley glaciers (Fig. 1).

Mt. Melbourne is a late Cenozoic intraplate volcano, located ~40 km northeast of Jang Bogo Station (Fig. 1). The volcano is quiescent with fumarolic activity at the summit, which is 2732 m above sea level. The ground temperature on the summit is over 25°C and in some places too hot to touch (Nathan and Schulte, 1967), and a thematic mapper Landsat satellite study suggests anomalously higher surface temperatures (Mazzarini and Salvini, 1994). The most recent eruptions
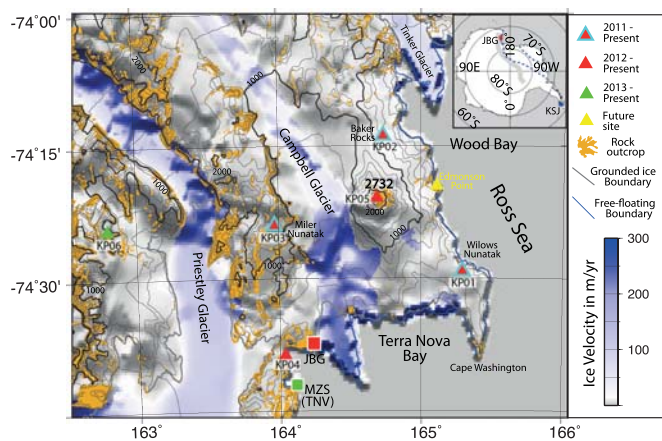
▲ **Figure 1.** The Mt. Melbourne area, showing the seismic stations, topography, and ice velocity. The digital elevation model from Bamber *et al.* (2009) overlies the ice velocity data from Rignot *et al.* (2011). The boundary of grounded ice (gray line) and the free-floating boundary (blue line) are extracted from Bindschadler *et al.* (2011). The seismic stations are represented by triangles of different colors, according to the year of installation. Inset map: dotted blue lines indicate the boundaries of the West Antarctic rift system, and the gray line represents the Transantarctic Mountains (TAM). KSJ, King Sejong Station; JBG, Jang Bogo Station; MZS, Mario Zucchelli Station; and TNV, Italian broadband seismic station in MZS.

took place between 1862 and 1922, based on the depth of ash layers buried in ice cliffs and snow accumulation rates determined by deuterium/hydrogen analysis (Lyon, 1986). Seismic observations were recorded at the end of 1990 by the Italian "Programma Nazionale di Ricerche in Antartide," involving four stations equipped with adjustable short-period seismometers (Teledyne Geotech model S-13), and two of these were three-component stations. In the continuous data recorded by the seismic network, several long-period local events were observed on the eastern slope of Mt. Melbourne, associated with the movement of magmatic fluids or the result of fracturing processes in a medium transitioning between brittle and plastic behavior (Gambino and Privitera, 1996). Other short-term temporary seismic stations were deployed in TNB and the Mt. Melbourne volcanic area during both Antarctic winter seasons in 1993 and 1994 (Di Bona *et al.*, 1997) and in southern Victoria Land along the ACRUP1 Geotraverse for 20 days in January 1994 (Pondrelli *et al.*, 1997). The Moho depth and upper-mantle anisotropy were studied by the receiver function and *SKS*- and *S*-wave splitting with short-term data sets, and the results showed the presence of seismic velocity anomalies and anisotropy in the area of Mt. Melbourne (Di Bona *et al.*, 1997; Pondrelli *et al.*, 1997; Pondrelli and Azzara, 1998).

INSTRUMENTATION AND DEPLOYMENT OF KPSN@TNB

As described in previous studies, there are many active geophysical features, such as long-period earthquakes involving magmatic fluids in Mt. Melbourne (Gambino and Privitera, 1996), extensions in the Ross Sea rift (e.g., Ben-Avraham *et al.*, 1998; Berg *et al.*, 1989; Davey and Brancolini, 1997), and fast ice movements in the Campbell and Priestley glaciers (Rignot *et al.*, 2011). Before building Jang Bogo Station, we had decided to deploy seismic stations to observe ground movements due to seismic and volcanic activities and interactions between ice movement and its energy release. First, four broadband stations were installed that consisted of a Nanometrics Trillium compact sensor and the Taurus data acquisition system (DAS) during the Antarctic summer of 2010–2011. Initially, we designed separate DAS and power enclosures for each station and planned to change the battery enclosure only after one year of operation. For operation, the Taurus DAS has two recording modes: communications and buffered modes. In the buffered mode, the average power consumption is ~750 mW when Taurus writes data onto a Compact Flash card at ~30 min intervals for three channels at 100 samples per second with the Global Positioning System Duty Cycle mode configured to automatic (Nanometrics, 2010a). In communications mode, it consumes more power, up to ~2.3 W, than in buffered mode. The Trillium Compact sensor consumes ~160 mW with a low seismic signal and ~1 W during power start-up (Nanometrics, 2010b). In buffered mode, at least ~570 A were needed for one-year operation at 14 V d.c. The actual capacity of a lithium battery pack will drop by ~50% of the nominal capacity in cold environments down to −30°C, and we prepared sufficient battery pack to operate the stations with 1440 A for one year. During the Antarctic summer field season in 2011–2012, we retrieved the first year-round continuous data from stations KP01, KP02, and KP03 and installed a new station on the summit of Mt. Melbourne (KP05) with a Q330 DAS and Trillium 240. Station KP04, installed in January 2011, did not work properly due to a power failure just after its installation, so it was reinstalled at a site closer to Jang Bogo Station in December 2012.

STATION NOISE LEVELS AND DATA QUALITY

After retrieving data, we checked the variation in input voltages and sensor currents with temperature. Figure 2 shows the variation in DAS with temperature at each station and sensor currents drawn by the Trillium Compact. We encountered an unusual phenomenon at stations KP02 and KP03; the electric sensor currents exceeded 25 mA when the DAS temperature was less than −20°C at KP02 in 2011 and at KP03 between 2011 and 2013. To evaluate the performance of the stations, we calculated the noise power spectral density (PSD; McNamara and Buland, 2004). McNamara and Buland (2004) invented a noise estimation method using a probability density function (PDF) to examine the PSD distribution. In this procedure, we need not remove all transient signals (such as earthquakes, system artefacts, or instrumental glitches) because they are discriminated due to their lower probability, and the power values with high probability of occurrence in each period represent the stationary background ambient noise at each station.
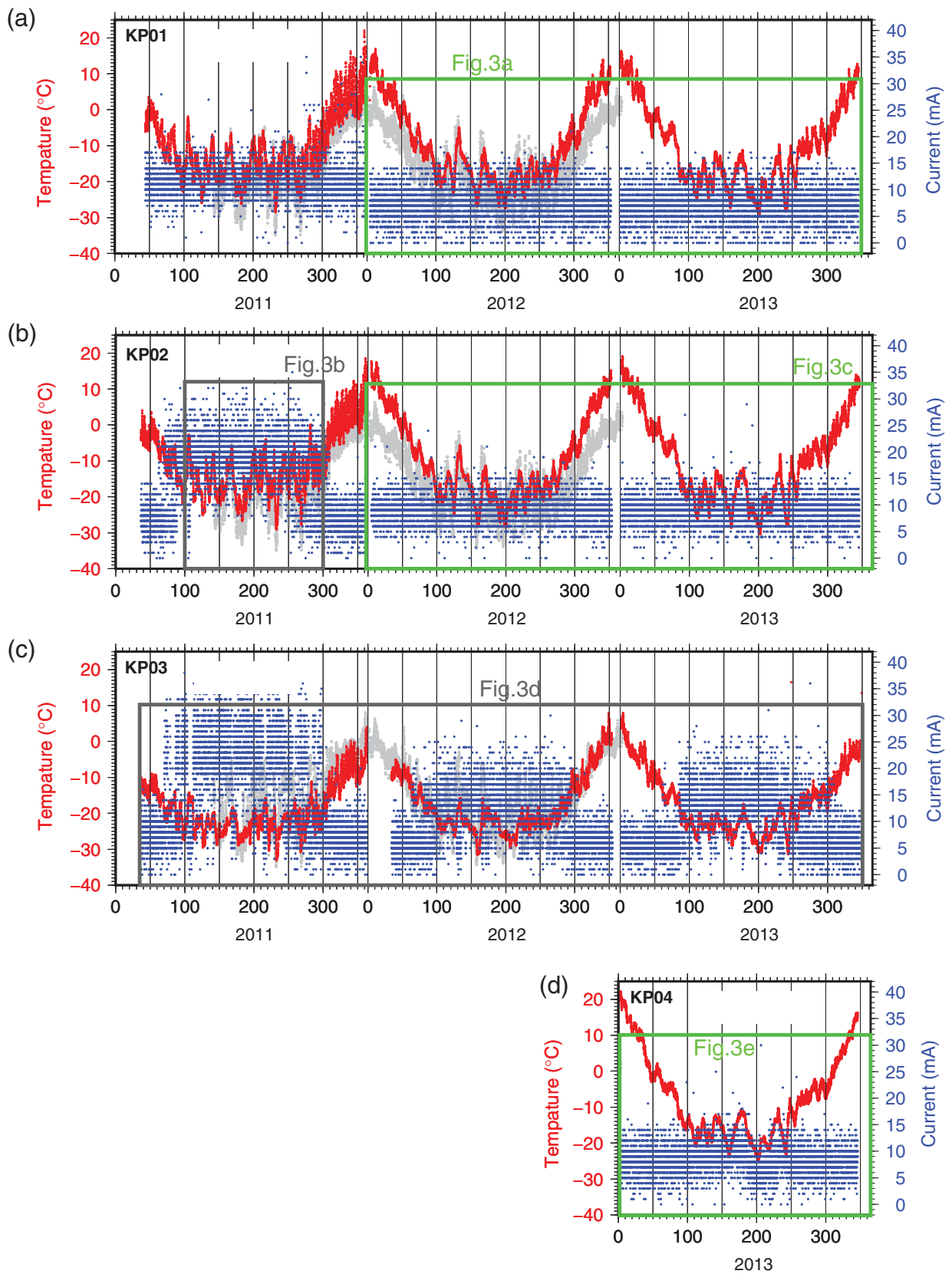
▲ **Figure 2.** Temperature and sensor-current variations for (a) KP01, (b) KP02, (c) KP03, and (d) KP04. The temperature variation is presented with red dots in degrees Celsius, and the sensor-current variation is indicated by blue dots in milliamperes. Gray dots are the temperature variation observed on the autonomous weather station (AWS) at Jang Bogo Station. Black and green boxes indicate the time windows of high-sensor current and normal current periods for computing the power spectral densities (PSDs) in Figure 3.
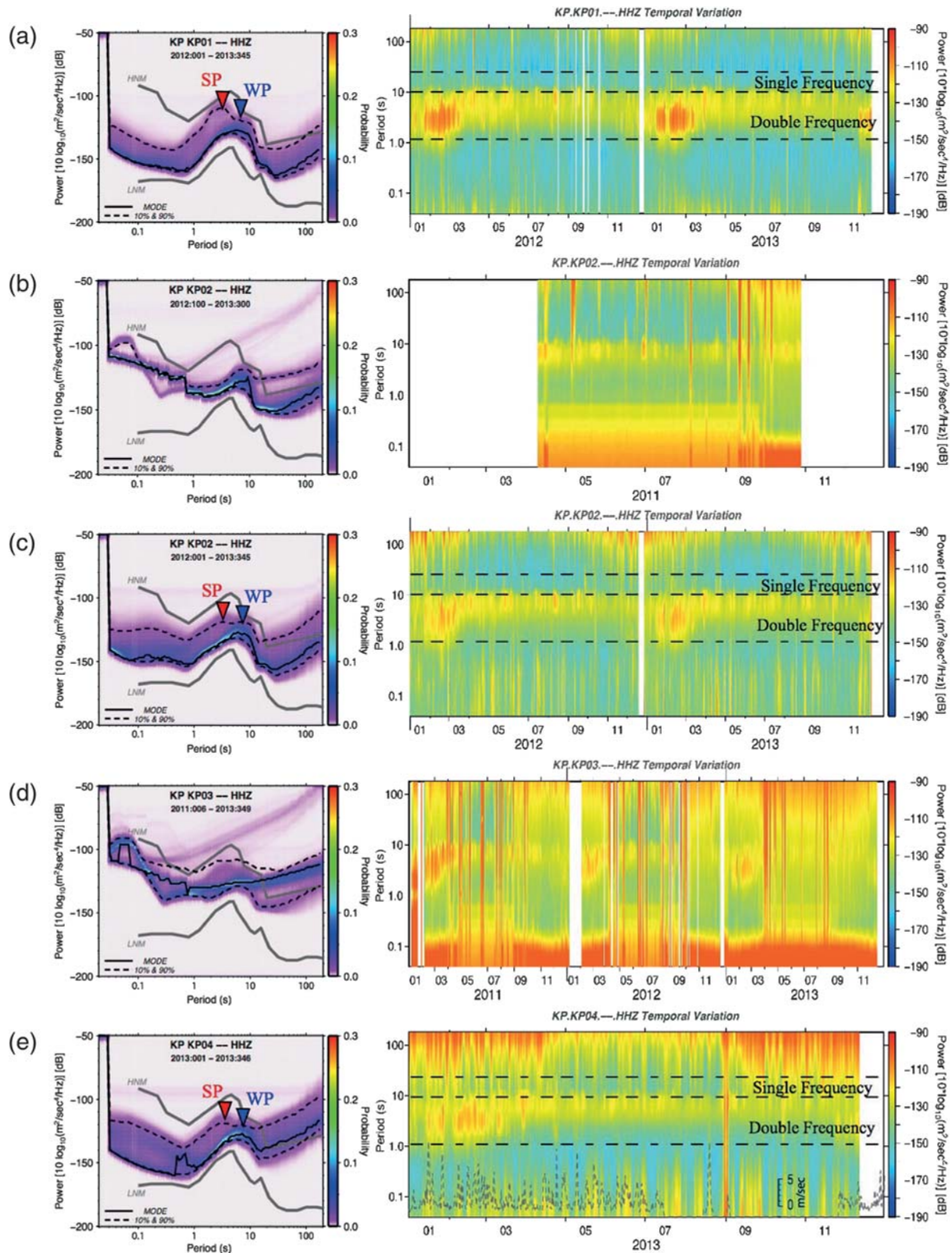
▲ **Figure 3.** (Left) Distribution of PSDs (probability density function, PDF) and (right) temporal variation of seismic noise PSDs of (a) KP01, (b, c) KP02, (d) KP03, and (e) KP04 for each time window in Figure 2. In the left plots, the black solid line and upper/lower black dotted lines represent the mode and 90th/10th percentiles of the computed PDFs, respectively. Summer (SP) and winter peaks (WP) are shown as inverted red and blue triangles on the PDF panel in (a)–(c). A gray dashed line on PSD in (e) shows the wind speed variation observed on an AWS at the Jang Bogo Station construction site.

The PDF and temporal variation plots of the seismic noise PSD of vertical recordings for four stations (KP01, KP02, KP03, and KP04) are shown in the left and right columns of Figure 3, respectively. To verify the abnormally high current effect on the seismic recordings during the Antarctic winter at stations KP02 and KP03 (Fig. 2b,c), the high (Fig. 3b,d) and normal current parts (Fig. 3c) of the PSDs were calculated separately for comparison. During the period of normal current,

all stations except KP03 showed relatively stable noise condition with 20–30 dB of broad separations between the 10th and 90th percentiles throughout the entire frequency band (Fig. 3a, c,e), which reflect significant diurnal and seasonal noise variations in this region, as is evident in the temporal PSD plots in Figure 3. The seasonal variation is more pronounced in the microseismic (2–20 s) and long-period band (> 20 s), than in the short period (Fig. 3a). The daily fluctuation pattern,
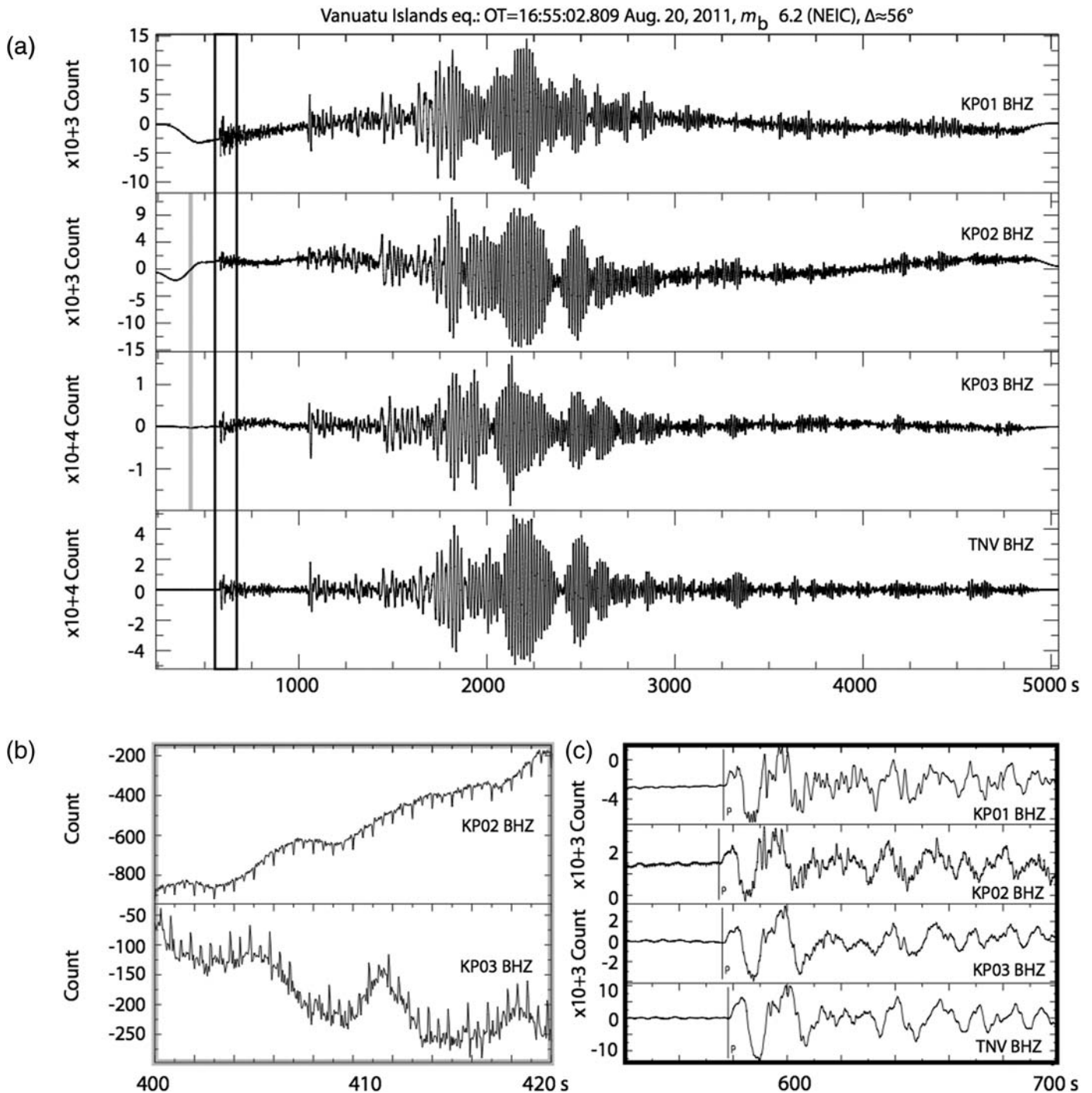
▲ **Figure 4.** An example of vertical-component waveforms observed at the KPSN@TNB and TNV stations. Gray and black boxes in (a) represent time windows for noise, and the first *P*-wave arrival parts are magnified in (b) and (c).

however, is distinctive in the short-period band (1–0.2 s). The daily variation in the short-period noise can be attributed to strong local winds (Fig. 3e) (Groos, 2010; Withers *et al.*, 1996) in the Antarctic region, which easily influence an exposed sensor vault on the surface. The microseismic energy is higher during the Antarctic summer, and the energy decreases during the Antarctic winter at all stations, although there is local variation in the average energies and duration. Seasonality of the energy is readily observable in the temporal PSD plots (right in Fig. 3a,c,e). This variation is more distinct in the double-frequency band (2–10 s) than in the single-frequency band (10–16 s). We also observed a shift in the double-frequency peak to a longer period in the Antarctic winter (WP to SP in the PDF plots in Fig. 3a,c,e). Smearing in the PDF plots at a period of $2 \sim 3$ s is associated with this frequency shift. The seasonal variation of the long-period noise, high in summer and low in winter, appears well correlated with microseismic energy changes. Stutzmann *et al.* (2009) and Grob *et al.* (2011) suggested this seasonal variation at coastal stations in Antarctica can be explained by sea-ice extension and concentrations that vary seasonally and interannually.

Stations KP02 and KP03 show an anomalous step-like response at high frequencies (> 1 Hz) and a bimodal distribution of the PSD for all frequency bands during the periods of abnormal high sensor current (Fig. 3b,d). The instruments installed at KP02 and KP03 were purchased at the same time in October 2010, and their serial numbers were 2664 and 2700, which indicates they were produced during the same period. When we retrieved the first data and maintained the stations in December 2011, we replaced the Taurus DAS and backed up the data at the field base camp at Mario Zucchelli Station. The Taurus DAS taken from the former station was reinstalled at the next station. The Taurus at KP02 was replaced with a new one, and the original was moved to KP03. After returning the data to KOPRI, we found this high sensor current problem and could not decide whether it was caused by malfunction of the Trillium compact sensor, lithium batteries, or Taurus DAS. Station KP02 showed a stable response after replacing the Taurus DAS at the beginning of 2012 (Fig. 3c), while station KP03, which received the Taurus from KP02, still suffered from the anomalous response problem. Therefore, the Taurus seemed to have caused this problem, and the DAS, with serial numbers from 2600 to 2700 (produced in 2010), might be less tolerant of the cold environment. The PSD distributions for stations KP02 and KP03 (Fig. 3b,d) are discrete, implying that the cold environment permanently damaged the DASs.

The waveforms during the period of high sensor currents at KP02 and KP03 were contaminated by electric pulse-like noise almost every half second. Figure 4 shows examples of vertical-component waveforms from a teleseismic event occurring near the Vanuatu Islands on 20 August 2011. The whole waveforms were recorded, including body and surface waves, at stations KP01, KP02, KP03, and TNV. Recurrent electric pulses with an amplitude of ~50 counts were seen in the ambient noise before the first *P* waves arrived at KP02 and KP03

(Fig. 4b). Although the data recorded at KP02 in 2011 and at KP03 between 2011 and 2013 are unreliable for converting to actual ground displacements, as the signals are good enough to distinguish the seismic phases, as clearly shown in Figure 4c, then at least the travel times of the selected phase can be used for further research.

SUMMARY

The seismic network KPSN@TNB was installed in January 2011 in the vicinity of Jang Bogo Station. It is the first Korean year-round seismic network to monitor the volcanic activity of Mt. Melbourne and nearby ice movements. We successfully retrieved continuous data from 2011 to 2013, although the data recorded at KP02 and KP03 were contaminated by abnormally high sensor currents. They might be due to faults in the Taurus DASs produced in 2010. The waveforms during the high-sensor current periods were contaminated by electronic pulses every 0.5 s with an amplitude of ~50 counts. The Taurus DASs at KP02 and KP03 were replaced by new ones in December 2011 and December 2013, respectively. Though we failed to retrieve data from KP06 in this season because of harsh weather during the 2013–2014 field season, KPSN@TNB currently consists of six broadband seismic station, with one additional station installed at Edmonson Point during the 2014–2015 field season (Fig. 1).

DATA AND RESOURCES

The seismic data used in this study were collected as part of the Korea Polar Seismic Network installed by Korea Polar Research Institute (KOPRI), and they can be shared for collaborative work with KOPRI Extreme Geophysics Group. All figures in this article were generated by the Generic Mapping Tools 4.5.8 (www.soest.hawaii.edu/gmt, last accessed June 2012; Wessel and Smith, 1998). ⬧

ACKNOWLEDGMENTS

REFERENCES

Bamber, J. L., J. L. Gomez-Dans, and J. A. Griggs (2009). A new 1 km digital elevation model of the Antarctic derived from combined satellite radar and laser data—Part 1: Data and methods, *Cryosphere* **3**, 101–111.

Behrendt, J. C. (1999). Crustal and lithospheric structure of the West Antarctic rift system from geophysical investigations—A review, *Global Planet. Change* **23**, 25–44.

Behrendt, J. C., and A. Cooper (1991). Evidence of rapid Cenozoic uplift of the shoulder escarpment of the Cenozoic West Antarctic rift system and a speculation on possible climate forcing, *Geology* **19**, 315–319.

Ben-Avraham, Z., M. Busetti, and G. Spadini (1998). Transform-normal extension in the Victoria Land basin (Antarctica), *Rend. Fis. Acc. Lincei* **9**, 257–269.

Berg, J. H., R. J. Moscati, and D. L. Herz (1989). A petrologic geotherm from a continental rift in Antarctica, *Earth Planet. Sci. Lett.* **93,** 98–108.

Bindschadler, R., H. Choi, A. Wichlacz, R. Bingham, J. Bohlander, K. Brunt, H. Corr, R. Drews, H. Fricker, M. Hall, R. Hindmarsh, J. Kohler, L. Padman, W. Rack, G. Rotschky, S. Urbini, P. Vornberger, and N. Young (2011). Getting around Antarctica: New high-resolution mappings of the grounded and freely-floating boundaries of the Antarctic ice sheet created for the International Polar Year, *Cryosphere* **5,** 569–588.

Danesi, S., and A. Morelli (2001). Structure of the upper mantle under the Antarctic Plate from surface wave tomography, *Geophys. Res. Lett.* **28,** 4395–4398.

Davey, F. J., and G. Brancolini (1997). The Late Mesozoic and Cenozoic structural setting of the Ross Sea region, in *Geology and Seismic Stratigraphy of the Antarctic Margin*, American Geophysical Union, Vol. 68, 167–182.

Di Bona, M., A. Amato, R. Azzara, G. B. Cimini, D. Colombo, and S. Pondrelli (1997). Constraints on the lithospheric structure beneath the Terra Nova Bay area from teleseismic *P* to *S* conversions, in *International Symposium on Antarctic Earth Sciences*, Siena, Italy, Vol. 7, 1087–1093.

Faccenna, C., F. Rossetti, T. W. Becker, S. Danesi, and A. Morelli (2008). Recent extension driven by mantle upwelling beneath the Admiralty Mountains (East Antarctica), *Tectonics* **27,** doi: 10.1029/2007TC002197.

Fitzgerald, P. G., M. Sandiford, P. J. Barrett, and A. J. W. Gleadow (1986). Asymmetric extension associated with uplift and subsidence in the Transantarctic Mountains and Ross Embayment, *Earth Planet. Sci. Lett.* **81,** 67–78.

Gambino, S., and E. Privitera (1996). Mt. Melbourne volcano, Antarctica: Evidence of seismicity related to volcanic activity, *Pure Appl. Geophys.* **146,** 305–318.

Grob, M., A. Maggi, and E. Stutzmann (2011). Observations of the seasonality of the Antarctic microseismic signal, and its association to sea ice variability, *Geophys. Res. Lett.* **38,** L11302, doi: 10.1029/2011GL047525.

Groos, J. C. (2010). Broadband seismic noise: Classification and Green's function estimation, in *Faculty of Physics*, von der Fakultät für Physik des Karlsruher Instituts für Technologie, Karlsruhe, 155.

Hong, J. K., S. Nam, J. Lee, B. Lee, H. Jung, J. Jung, H. Shin, H. Yoon, S. Jang, M. Park, Y. Kang, H. Lee, S. Huh, C. Kang, J. Lee, H. Yoo, and C. Hong (2005). Feasibility study for the construction of the new Antarctic station, Ministry of Maritime Affairs and Fisheries, 172 pp.

Lawrence, J. F., D. A. Wiens, A. A. Nyblade, S. Anandakrishnan, P. J. Shore, and D. Voigt (2006). Rayleigh wave phase velocity analysis of the Ross Sea, Transantarctic Mountains, and East Antarctica from a temporary seismograph array, *J. Geophys. Res.* **111,** doi: 10.1029/2005JB003812.

Lee, Y. J., N. Moon, T. H. Ro, D. J. Chun, Y. H. Kwon, J. Y. Kim, J. Choi, Y. Kim, J. H. Kim, and J. Lee (2012). Final Comprehensive Environmental Evaluation, Construction and operation of the Jang Bogo Antarctic Research Station, Terra Nova Bay, Antarctica, 153 pp., available at http://eng.kopri.re.kr/home/contents/images/contents/e_5310000/Final_CEE_Jang_Bogo_ROK.pdf (last accessed January 2014).

Lyon, G. L. (1986). Stable isotope stratigraphy of ice cores and the age of the last eruption at Mount Melbourne, Antarctica, *New Zeal. J. Geol. Geophys.* **29,** 135–138.

Mazzarini, F., and F. Salvini (1994). Contribution to geothermal survey by spectral analysis of TM Landsat satellite data in Mt. Melbourne area, *Northern Victoria Land (Antarctica), Terra Antarctica* **1,** 104–106.

McNamara, D. E., and R. P. Buland (2004). Ambient noise levels in the continental United States, *Bull. Seismol. Soc. Am.* **94,** 1517–1527.

Nanometrics (2010a). *Taurus Portable Seismograph User Guide*, Nanometrics, Ontario, Canada, 208.

Nanometrics (2010b). *Trillium Compact Seismometer User Guide*, Nanometrics, Ontario, Canada, 65.

Nathan, S., and F. J. Schulte (1967). Recent thermal and volcanic activity on Mount Melbourne, northern Victoria Land, Antarctica, *New Zeal. J. Geol. Geophys.* **10,** 422–430.

Pondrelli, S., and R. Azzara (1998). Upper mantle anisotropy in Victoria Land (Antarctica), *Pure Appl. Geophys.* **151,** 433–442.

Pondrelli, S., A. Amato, M. Chiappini, G. B. Cimini, D. Colombo, and M. Di Bona (1997). ACRUP1 Geotraverse: Contribution of teleseismic data recorded on land, in *The Antarctic Region: Geological Evolution and Processes*, C. A. Ricci (Editor), Terra Antartica Publication, Siena, 631–635.

Rignot, E., J. Mouginot, and B. Scheuchl (2011). Ice flow of the Antarctic ice sheet, *Science* **333,** 1427–1430.

Rocchi, S., P. Armienti, M. D'Orazio, S. Tonarini, J. R. Wijbrans, and G. Di Vincenzo (2002). Cenozoic magmatism in the western Ross Embayment: Role of mantle plume versus plate dynamics in the development of the West Antarctic rift system, *J. Geophys. Res.* **107,** 2195.

Smith, A. G., and D. J. Drewry (1984). Delayed phase change due to hot asthenosphere causes Transantarctic uplift? *Nature* **309,** 536–538.

Stutzmann, E., M. Schimmel, G. Patau, and A. Maggi (2009). Global climate imprint on seismic noise, *Geochem. Geophys. Geosyst.* **10,** Q11004, 10.1029/2009GC002619.

ten Brink, U., and T. Stern (1992). Rift flank uplifts and Hinterland basins: Comparison of the Transantarctic Mountains with the Great Escarpment of southern Africa, *J. Geophys. Res.* **97,** 569–585.

ten Brink, U. S., R. I. Hackney, S. Bannister, T. A. Stern, and Y. Makovsky (1997). Uplift of the Transantarctic Mountains and the bedrock beneath the East Antarctic ice sheet, *J. Geophys. Res.* **102,** 27,603–27,621.

Wessel, P., and W. H. F. Smith (1999). New, improved version of Generic Mapping Tools released, *Eos Trans. AGU* **79,** no. 47, 579 pp.

Withers, M. M., R. C. Aster, C. J. Young, and E. P. Chael (1996). High-frequency analysis of seismic background noise as a function of wind speed and shallow depth, *Bull. Seismol. Soc. Am.* **86,** 1507–1515.

Yongcheol Park
Hyun Jae Yoo
Won Sang Lee
Joohan Lee
Yeadong Kim
Sang-Hyun Lee
Dongseob Shin
Hadong Park
Korea Polar Research Institute
26 Songdomirae-ro
Yeonsu-gu, Incheon 406-840, Korea
ypark@kopri.re.kr

Published Online 1 October 2014